A parametric study of an offshore concrete pile under combined loading conditions using finite element method

J.A. Eicher , H. Guan[1] and D. S. Jeng
School of Engineering, Griffith University Gold Coast Campus, QLD9726, Australia
[1] *Corresponding author, E-mail: h.guan@mailbox.gu.edu.au*

Received 11 Sep 2001; revised 28 Apr 2002; accepted 1 May 2002.

ABSTRACT

Offshore piles are commonly used as foundation elements of various offshore structures, especially large structures such as Tension Leg Platforms (TLP). The stress distribution within such a large structure is a dominant factor in the design procedure of an offshore pile. To provide a more accurate and effective design, a finite element model is employed herein to determine the stresses and displacements in a concrete pile under combined structural and wave loadings. The vertical structural load is essentially a static load, while the lateral wave loading fluctuates in time domain and is directly affected by the incident wave angle. The parametric study will consist of varying certain parameters of the pile to study the effects of the stress distribution under various combinations of structural and wave loadings.

KEYWORDS

Offshore foundations, concrete pile, finite element analysis, wave load, wave-structure interaction.

1. Introduction

Concrete piles are common structural foundation elements used to support offshore structures such as bridges, oil-rigs, and floating airports. The use of offshore structures is still a fairly new technique and there is still much research to be done in this field. The loading of an offshore structure consists of two components: vertical structural loads and lateral wave loads. The combinations of these two loading components have a significant impact on how the pile reacts and the way the stresses are distributed throughout the pile.

Wave forces on the offshore structures are the major contribution to the total forces experienced by such structures, particularly in rough weather. The calculation of the wave loads on vertical cylinders is always of major concern to ocean engineers, especially recently when such studies are motivated by the need to build solid offshore structures in connection with oil and natural gas productions. The effects of various wave patterns on offshore piles have been investigated by numerous researchers in the past [1-5]. In addition, structural engineers have also conducted research on offshore piles, considering pile capacity [6] and the effects of the structural loads on offshore piles. However, little study on the effects of the combined wave and varying structural loads on the pile has been found in the literature.

The aim of this study is to investigate the effects of the combined loads on an offshore concrete pile and the effects of varying the pile parameters. The stress distributions within the offshore concrete pile will be estimated. The change in the stress distribution and displacement due to varying structural loads will also be studied through a parametric study.

2. Structural and Wave Loading

2.1 Dynamic Wave Pressure

Water depth and wave period are two essential wave parameters, which must be considered in the design of any coastal structure. When the relative water depth (water depth/wave length, *d/L*) is less than 0.5, it is classified as a shallow water wave [7]. In this paper, the three-dimensional short-crested waves are considered for the dynamic wave loading. Short-crested waves are created by winds blowing over the surface of the water and have a finite lateral extent. Zhu [4] concluded that a short-crested wave exerts a smaller dynamic force than a plane wave with the same wave number in the same direction of propagation. However, as the wave number of short-crested waves perpendicular to the propagation of the plane waves increases, the total wave load increases. The first-order solution of the short-crested wave loading proposed by Zhu [4] is used to calculate the wave load acting on the offshore concrete pile. The dynamic wave pressure at any point on the surface of the pile is given as [4]

$$p_d(a,\theta,z) = \frac{\gamma_w A}{2}\frac{\cosh k(z+d)}{\cosh kd}\, e^{-i\omega t}\sum_{m=0}^{\infty}\sum_{n=0}^{\infty}\varepsilon_m\varepsilon_n i^m Q_{mn}(a,\theta) \tag{1}$$

where p_d is the dynamic wave pressure acting on the pile, a is the radius of the pile, θ is the angle around the circumference of the pile where the wave load is being calculated, and z is the vertical depth from the surface of the water to the point where the wave load is being calculated. In Equation (1), γ_w is the unit weight of water, A is the amplitude of the waves being considered, k (=$2\pi/L$, L is the wavelength) is the wave number, and d is the total depth of water. Fig. 1 shows some of these variables. Also in Equation (1), i is equal to $\sqrt{-1}$, ω is the wave frequency, and t is the second of the wave period that the wave load is being calculated.

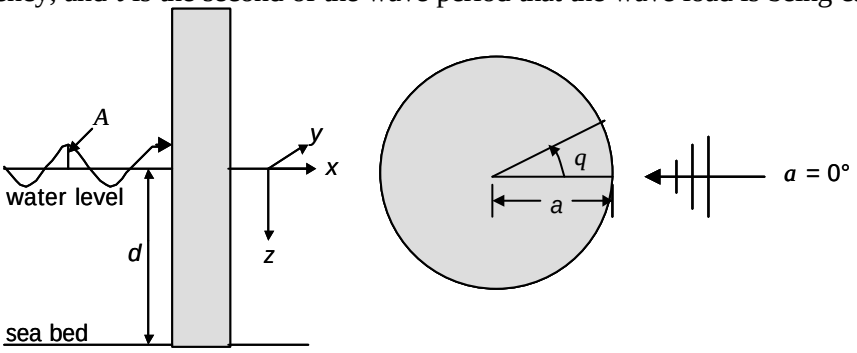

Fig. 1 Definition of variables.

In Equation (1), parameters ε_m, ε_n and $Q_{mn}(a,\theta)$ are defined as follows [4]

$$\varepsilon_m,\varepsilon_n = \begin{cases} 1 & \text{when } m,n = 0 \\ 2 & \text{when } m,n \neq 0 \end{cases} \tag{2}$$

$$Q_{mn}(a,\theta) = \left[J_m(k_x a)J_{2n}(k_y a) - A_{mn}H_{m+2n}(ka)\right]\cos(m+2n)\theta + \left[J_m(k_x a)J_{2n}(k_y a) - B_{mn}H_{|m-2n|}(ka)\right]\cos(m-2n)\theta \tag{3}$$

where

$$A_{mn} = \frac{k_x J'_m(k_x a)J_{2n}(k_y a) + k_y J_m(k_x a)J'_{2n}(k_y a)}{kH'_{m+2n}(ka)} \tag{4a}$$

$$B_{mn} = \frac{k_x J'_m(k_x a) J_{2n}(k_y a) + k_y J_m(k_x a) J'_{2n}(k_y a)}{kH'_{|m-2n|}(ka)} \tag{4b}$$

in which J represents the Bessel function of the first kind and H represents the Hankel function. In Equation (3), the wave number in the x- and y-directions, k_x and k_y, can be expressed as

$$k_x = k\cos\alpha \quad \text{and} \quad k_y = k\sin\alpha \tag{5}$$

where α is the incident wave angle.

2.2 Static Water Pressure

The pressure that normal hydrostatic water exerts on a vertical surface can be found easily, varying only with the depth of the water. The pressure can be calculated as follows [7]:

$$p_s = -\gamma_w z \tag{6}$$

where p_s is the static water pressure.

2.3 Vertical Structural Load

The structural load is a vertical pressure load and is determined by using structural/water pressure ratios. The structural loads applied to the pile range from a ratio of zero, i.e. without structural load, to 10 times the static water pressure. Fig. 2 shows all the loads acting together on the pile.

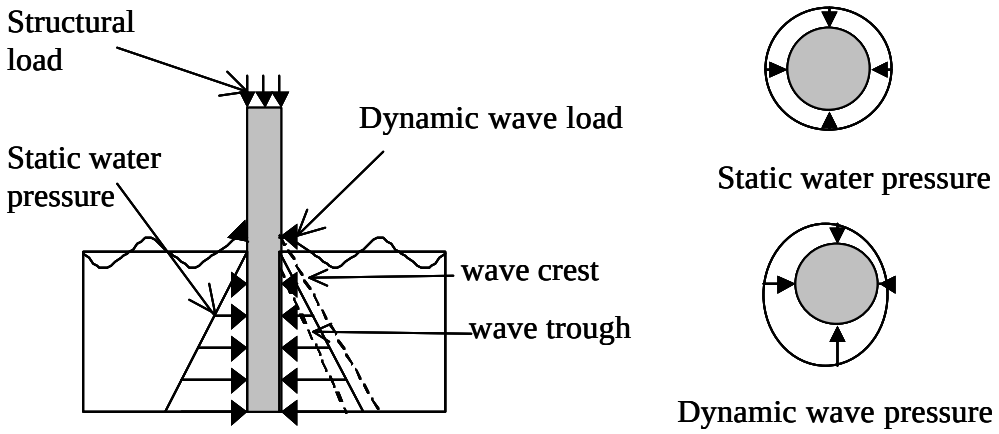

Fig. 2 Loading on the offshore pile

3. Numerical Study

The finite element analysis software, STRAND7 [8], is used in this study. The pile is modelled using 20-node brick elements except for the inner ring where 15-node wedge elements are used. A fixed support condition is provided at the points where the pile is embedded into the ocean bed. For the concrete pile, the Young's modulus is 28,600 MPa and the Poisson's ratio is 0.2.

3.1 Convergence of Model

Before finalising the model, a convergence study is performed under the structural and the static wave pressure to determine the most appropriate mesh size to use. Based on the results from the convergence study, the calculated loads are then applied and the analyses are performed to find the resulting stress and strain distributions as well as the resulting displacements.

Two series of convergence studies are performed. The first convergence test is to refine the mesh vertically above and below the surface water level. The second convergence test is to refine the mesh on the cross-section of the pile. In total, fifteen different models are used for the tests, including three variations of the mesh in the vertical direction on the surface water level (Models X, Y, and Z), and for each of these three models, five variations of mesh on the cross-section (4, 6, 8, 10, and 12 rings). The details of the different mesh schemes are shown in Fig. 3. It should be noted that due to the nature of a 20-node brick, the side nodes of each brick element form an intermediate ring.

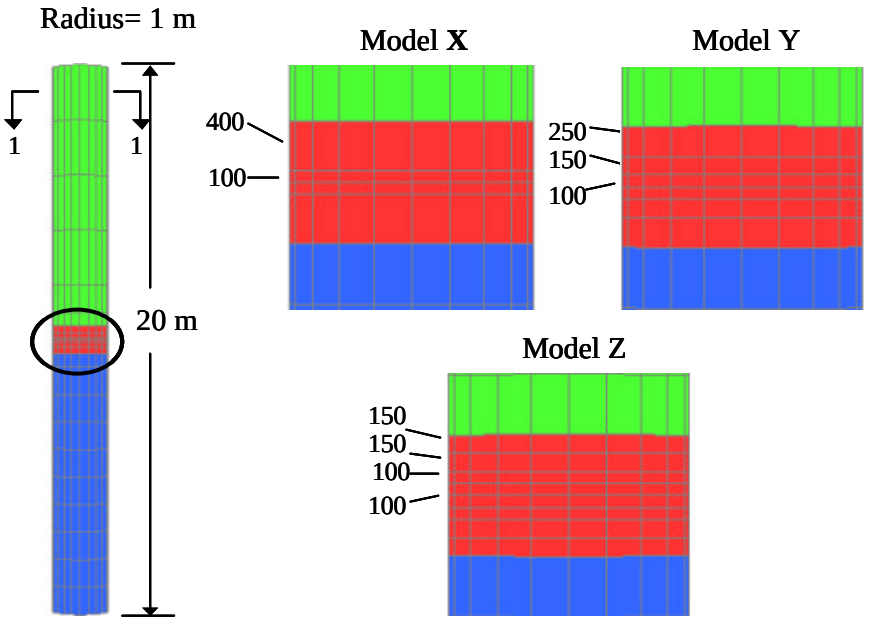

(a) control pile model and vertical mesh refinement at surface water level

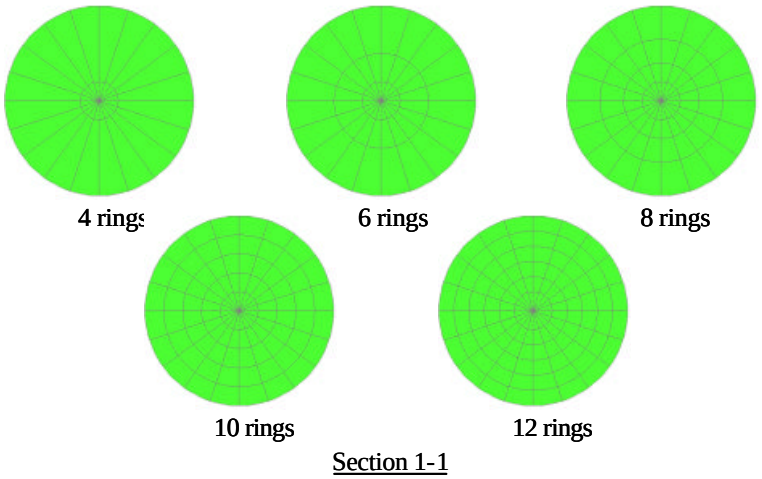

(b) mesh refinement through cross-section

Fig. 3 Pile models used for convergence study

The typical results of the convergence study are presented in Fig. 4 Fig. 4a presents the distribution of the von Mises stress at point A (refer to Fig. 5) versus the number of rings for Models X, Y, and Z. As can be seen in Fig. 4a, the solution starts to converge when the 6-ring model is adopted, with the change in slope between the 8, 10, and 12 ring models being very small. Fig. 4b shows the vertical displacement at point A versus Models X, Y, and Z for all number of ring models. It can be noted that the convergence is achieved when Model Y is used.

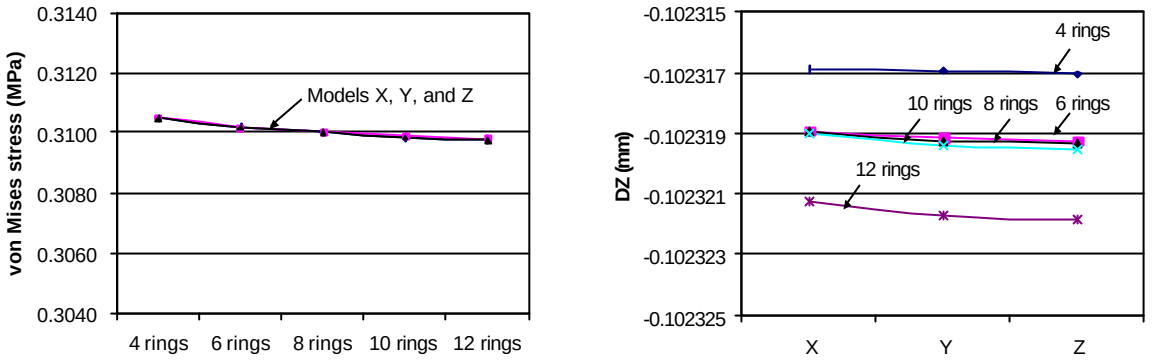

(a) von Mises stress at point A. (b) vertical displacement at point A.

Fig. 4 Results of the convergence study

Based on the convergence study, Model Y with six rings is selected to simulate the control pile. This mesh has 1320 bricks and 5505 nodes. The numerical analysis is then carried out to include the static water pressure, the dynamic wave loads, as well as the varying structural loads.

3.2 Effects of Combined Loading Conditions

After applying the loading conditions to the final model that is selected, the three-dimensional finite element analyses are performed. The results of these analyses show a significant difference in the stress distribution due to the different combination of the loads. Fig. 5a shows the stress distribution of the centre surface of the pile due to the structural load of 10 times the static water pressure. Under such loading conditions, the stress distribution is found to be symmetrical about the vertical central axis of the pile. The stress distribution due to the same structural load together with the dynamic wave loads, which is at the time two of a ten-second wave period (see Fig. 5b), illustrates how the stress concentrations change around the base of the pile. It should be noted that the location of the highest stress concentration varies over the period of a wave.

3.3 Ratio of Structural and Wave Loads

One of the major concerns of this study is to examine the effects of the combined loading on the offshore pile. To examine the effects of increased structural loads on the overall behavior of the pile, the total displacement of and the von Mises stress in the pile versus the ratio of structural load to static water pressure at the base of the pile are presented in Fig. 6. These results are taken at the same point A as shown in Fig. 5. Again, these results are generated from the analyses performed at time zero of a wave period of 10 seconds. Also, a wave height of one meter is considered. The ratio of structural to water pressure ranges from zero, with the pile having no structural load, to a structural load of 10 times the static water pressure at the base of the pile. Fig. 6 clearly indicates that the total displacements, as well as the stresses, increase linearly with the increasing structural load. The total displacement is the displacement resultant due to the components in the *x*-, *y*-, and *z*- directions. The total displacement increases at a slope of approximately 1/100 and the von Mises stress increases at a slope of approximately 3/100.

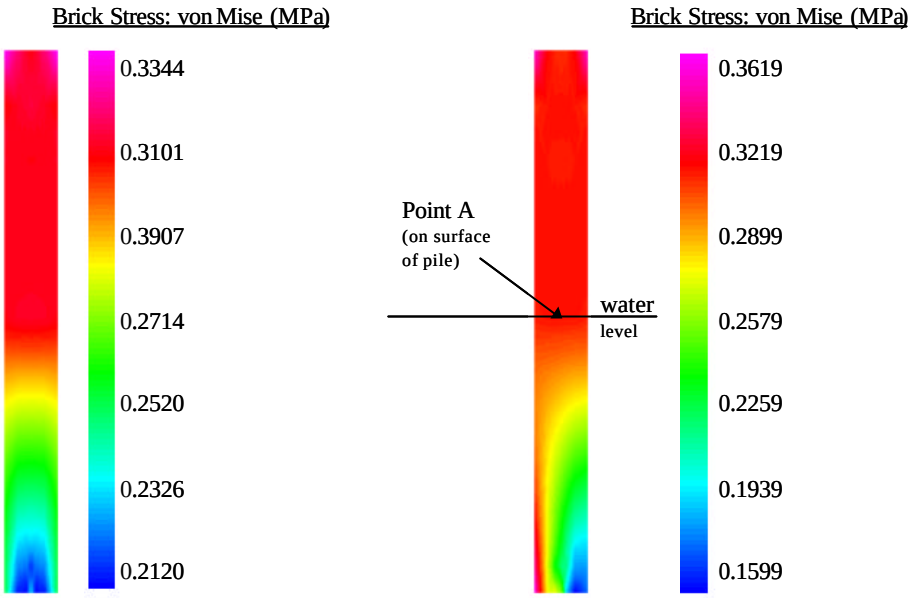

(a) combined structural load and static water pressure

(b) combined structural load and dynamic water pressure

Fig. 5 Contour of stress distribution due to combined structural load and (a) static water pressure and (b) dynamic wave pressure

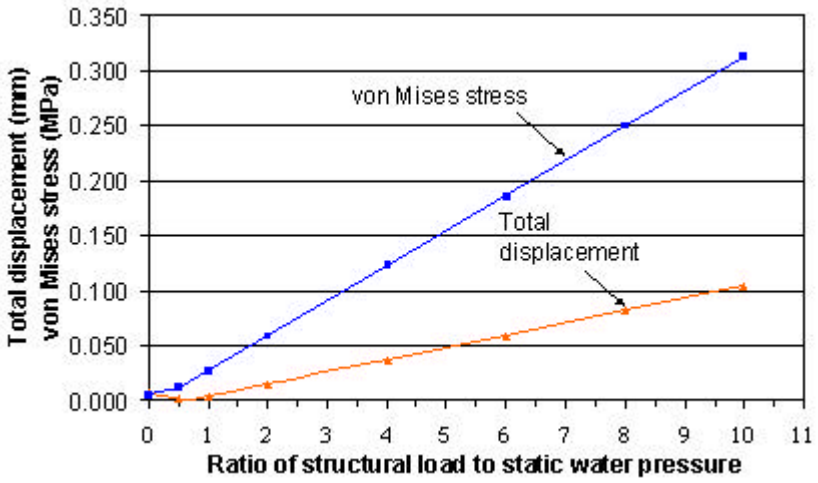

Fig. 6 Variation of von Mises stress and displacement under different structural and wave load ratios

To have a better understanding of the behavior over the entire height of the pile, Fig. 7 demonstrates the resulting total displacement and the von Mises stress under varying structural and wave load ratios. The results are taken at ten different locations with the same *x*- and *y*-coordinates on the surface of the pile. The locations are at intervals of two meters, beginning two meters above the base of the pile. The results are shown at time 0 of the 10-second control wave period. As seen in Fig. 7(a), the displacement basically increases linearly with the height of the pile, but there is a slight curvature to the relationship below the water surface at z/h equal to 0.5. With a structural load to static water pressure ratio of zero, the displacement is actually greater along the entire height of the pile than that when a vertical load of 0.5 times the static water pressure is applied. Increasing the ratio from 0.5 to 1, the total displacement then begins to exceed the total displacement with zero structural load at just over 2/3 the pile height.

Increasing the ratio again to 2, the total displacement exceeds that with zero structural load over the entire height of the pile. Continuing to increase the ratio up to 10, the displacement increases at equal increments at each of the ten locations. At the top of the pile, the displacement increases at approximately 0.0223 mm per unit increase of the ratio.

Similar results were taken for the von Mises stress, as shown in Fig. 7b. Similar to the displacement results, the von Mises stress is shown to be smaller up to a certain height when the ratio of the structural load to static water pressure increases up to 4 than when there is a zero structural load. At a ratio of 4, the height at which the stress begins to exceed a ratio of zero is about 4 meters. Also, the stress in the top half of the pile is significantly smaller up to a ratio of 4, this indicates that the wave loading is the more critical loading condition. However, after the ratio increases above four, the structural load then causes the stress in the top half of the pile to increase, therefore becoming more critical than at the base of the pile. The curves indicate that the stress remains constant above the surface water level up to just below the top of the pile, where the stress begins to significantly increase at ratios greater than 4.

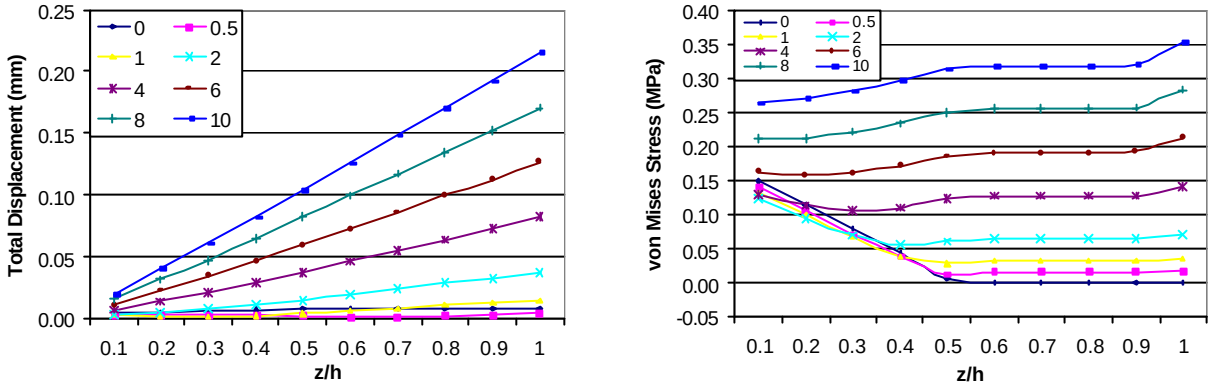

(a) change in total displacement. (b) change in von Mises stress.

Fig. 7 Results of increasing the structural to water pressure ratio at increasing heights on the pile.

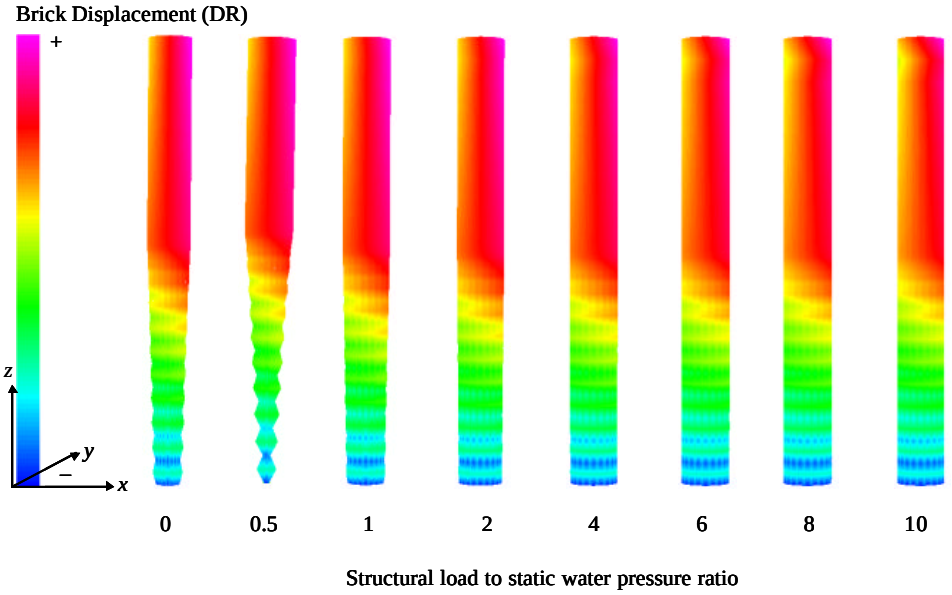

Fig. 8 Resulting deformation of the piles as the structural load to water pressure ratio increases. Displacement scale of 5%.

Fig. 8 illustrates the deformation of each pile under varying structural to wave load ratios by means of a contour plot of the displacement in the radial direction. The radial deformation presented in the Fig. is predicted under wave crests (i.e., t=0 second). The first three piles indicate that the deformation is significantly due to the deformation in the radial direction, which results from the static and dynamic water pressure. The second pile tapers even more than the first pile because the ratio of the vertical deformation to the lateral deformation is even smaller than the first pile, which has no structural load. This displacement response is also reflected in Fig. 7a, where the total displacement due to the 0.5 load ratio is even less than that due to a zero load ratio. The deformed shapes of the last five piles show very little lateral deformation which suggests that the increase in static load has little effect on the total displacement of the pile.

3.4 Parametric Study

In addition to investigating the effects of increasing structural and wave load ratios, a study is also undertaken to determine the effects of varying parameters of the control pile conditions. The parameters that are used include the pile radius (a), and the water depth (d). The control value used for the radius, a, is 1 meter with a water depth, d, of 10 meters. To complete the test for increasing water depths, a new model is generated to be more representative of a deep water situation. The control model is scaled 5 times the original dimensions, creating a 100-meter pile model with a 5-meter radius.

3.4.1 Effects of Varying Pile Radii

Four additional models are created to study the effects of increasing pile radii. The radii used are 0.5, 0.75, 1.25, and 1.5 meters with the control radius being 1 meter. The size of mesh used for this test is kept as close to the control pile as possible, reducing the number of rings for the 0.5 and 0.75 meter radius models and increasing the number of rings for the 1.25 and 1.5 meter radius models.

The first set of results is taken over the period of the wave at point A (see Fig. 5b). Fig. 9a shows the variation of stress by using a non-dimensional expression, dividing the von Mises stress by $\gamma_w H/2\cosh kd$, where H is the wave height. As seen in Fig. 9a, the stress remains fairly constant over the period of the wave for piles having different radii. However, as the radius increases the stress in the pile significantly decreases. The most significant decrease occurs when the pile radius increases from 0.5 meter to 0.75 meter. There is a second significant decrease in stress between the 0.75 meter and 1 meter radii piles, but then the decreases in stress are less significant indicating that a 1 meter or 1.25 meter radius is adequate for the loading condition applied.

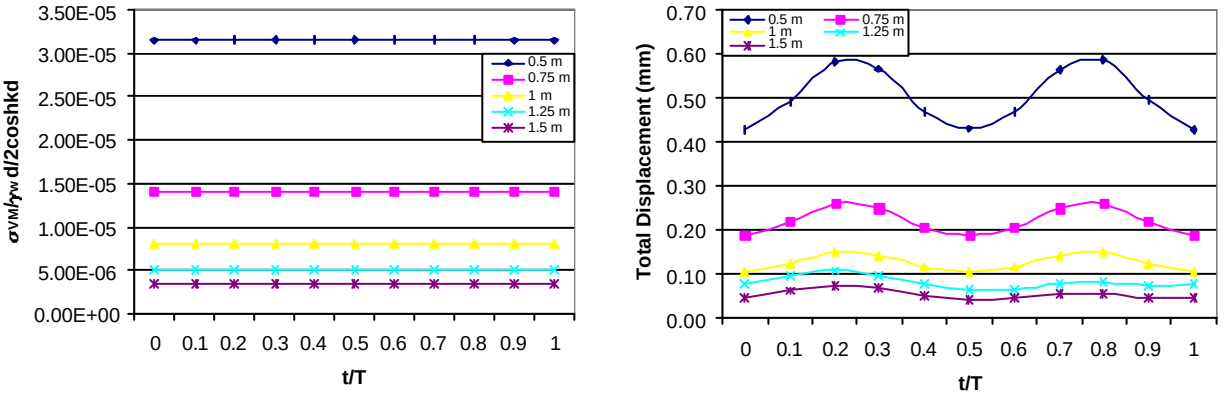

(a) change in von Mises stress (b) change in total displacement.

Fig. 9 Results at point A on the pile as the radius of the pile increases from 0.5 meters to 1.5 meters.

Similar decreases in displacement are shown in Fig. 9b as the total displacement in the *x*-, *y*-, and *z*-directions is plotted against the duration of the wave period. The sinusoidal curves indicate that the displacement peaks at 1/3 and 2/3 the wave period. Again, the reduction in displacement begins to level off when the radius reaches 1 meter or more.

The second set of results shown in Fig. 10 are taken over the height of the pile, at 2 meter intervals, with *y*- coordinates remaining the same and the *x*- coordinate being on the surface of the pile. Similar to the results shown for the structural load to static water pressure ratios, the total displacement increases linearly for each model, with the slope of the relationship decreasing as the radius increases. As before, the decrease in displacement levels off by the 1 meter control model.

The stress behavior over the height of the pile is also similar to Fig. 7b for the load ratio test in that the von Mises stress decreases to level off by the 1 meter and 1.25 meter models. The stress remains fairly constant, increasing slightly from the base of the pile up to the surface water level where the stress is constant up until just before the very top of the pile.

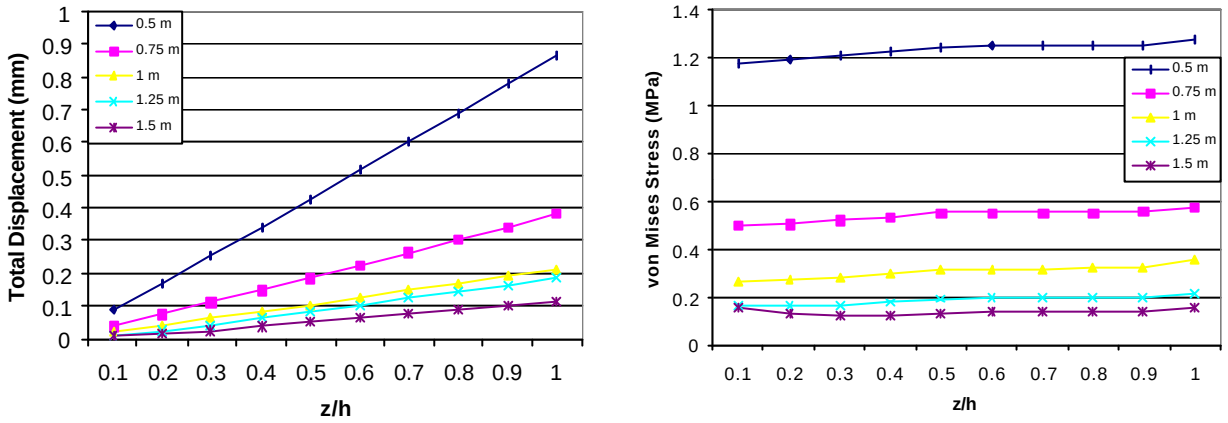

(a) change in total displacement (b) change in von Mises stress

Fig. 10 Results of increasing pile radius at increasing heights on the pile.

Fig. 11 illustrates the deformation of the piles of the increasing radii. The contour plot is based on the total displacement in the *x*-, *y*-, and *z*- directions at t = 2 seconds of the 10-second wave period, which is at the first peak of the sinusoidal wave. Displayed against the shadow of a non-deformed pile, the maximum displacement occurs at the top of the pile, but this maximum displacement decreases as the pile radius increases.

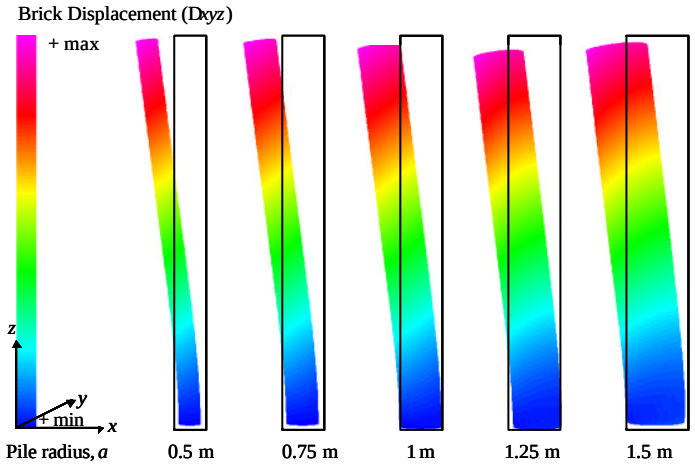

Fig. 11 Resulting deformation of the piles as the radius increases. Displacement scale of 10%.

3.4.2 Effects of Varying Water Depths

A 100-meter model is used to carry out a test to determine the effects of an increasing water depth on an offshore pile. The model used is five times the size of the original control model, having a 5-meter radius. The same mesh size is used, adding rings of bricks to the exterior of the original model. In addition, the loading parameters are kept at the original control values with a wave height of 1 meter, wave period of 10 seconds, and an angle of wave propagation of 15°. The structural load is also kept at the control ratio of 10 times the maximum static water pressure. The original model has a water depth of half the pile height, i.e. 50 meters, and the other water depths are chosen to be 30, 40, 60, and 70 meters.

Fig. 12 presents the stress and displacement over the height of the pile. Fig. 12a demonstrates the effect of the increasing water depths on the stress distribution. The stress decreases linearly at equal slopes for all models, levelling off at the surface water level where it then remains fairly constant, then increases slightly at the top of the pile.

Fig. 12b shows the total displacement of the pile as the water depths increase. It can be seen that the curvature of the displacement variation is convex from the base of the pile up to the surface water level. Then the curvature changes to concave from the surface water level to the top of the pile. It should also be noted that once the water level rises above the mid-height of the pile, the displacement in the top of the column significantly increases, while it only slightly increases when the water level is at or below the mid-height of the pile.

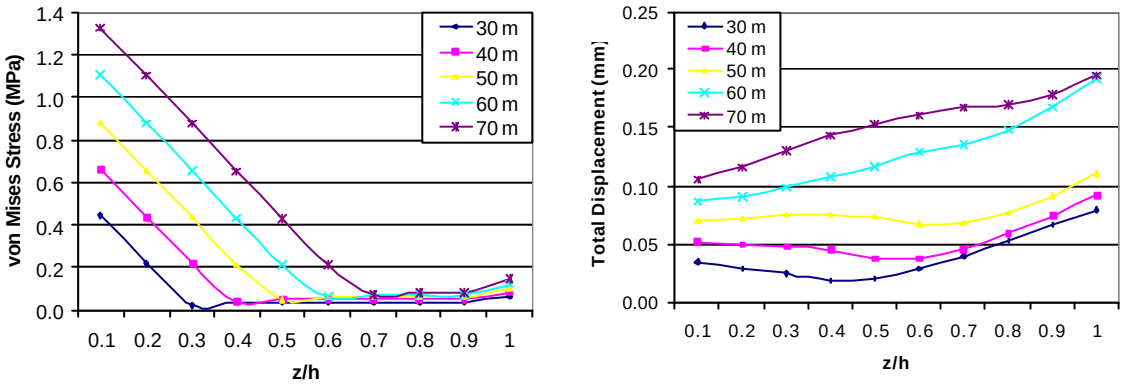

(a) change in von Mises stress. (b) change in total displacement.

Fig. 12 Results of increasing the water depth on a 100 meter pile shown at increasing heights on the pile.

Fig. 13 shows the deformation of the 100-meter piles with different water depths. The contour plot shows the distribution of the von Mises stress throughout the deformed pile. The aqua section on each pile indicates the point at the surface water level where the change in curvature of the displacement shown in Fig. 12b takes place. The deformed piles are displayed again the shadow of a non-deformed pile to show the increasing deformation as the water level increases.

3.4.3 Effects of Original Model Over the Wave Period

To better understand the behavior of the pile, a study is completed to see how the 20-meter control model reacts to the control loading condition over the period of the wave. Again, the results are taken at ten different locations at 2-meter intervals over the height of the pile, beginning 2 meters from the base of the pile. These locations are on the surface of the pile with the same *x*- and *y*- coordinates.

Fig. 14a shows the total displacement at each point for each second of the wave period. At each of the ten locations, the displacement increases up to t=2 s of the 10-second wave period, then begins to fall back down. By the time t=5 s of the period, the displacement is equal to that at time zero, then begins to increase again until t=8 s. The peak displacement at each location is at t=8 s after which the displacement again falls back down by t=10 s, equal to the displacement at time zero and the cycle begins again.

A similar result is seen in Fig. 14b with the von Mises stress distribution. The stress above the surface water level remains constant throughout the wave period, but varies greatly towards the base of the pile. But similar to Fig. 14a, the von Mises stress begins the wave period at approximately 0.26 MPa, decreases down to 0.2 MPa by t=2 s of the wave period where it begins to increase again. By t=5 s, the stress is equivalent to time zero, but then the stress begins to increase in the second half of the wave period. By t=8 s, the stress reaches a maximum of about 0.34 MPa where it begins to decrease back down to the start by t=10 s, which is the beginning of a new cycle.

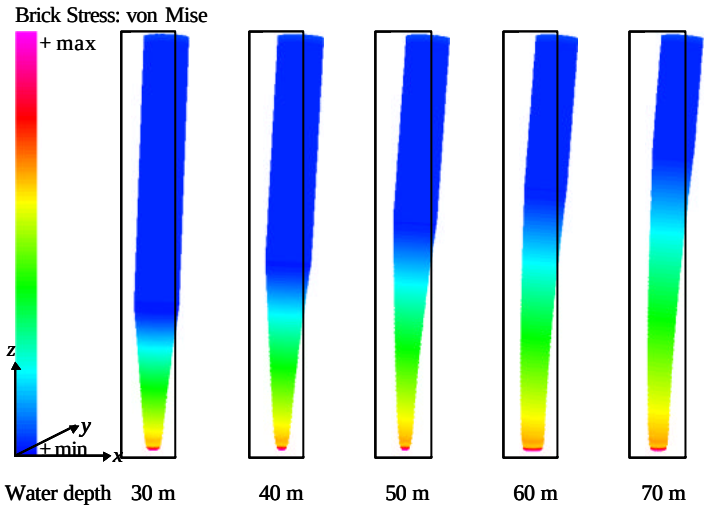

Fig. 13 Resulting deformation of the piles due to increasing the water height from 30 meters to 70 meters.

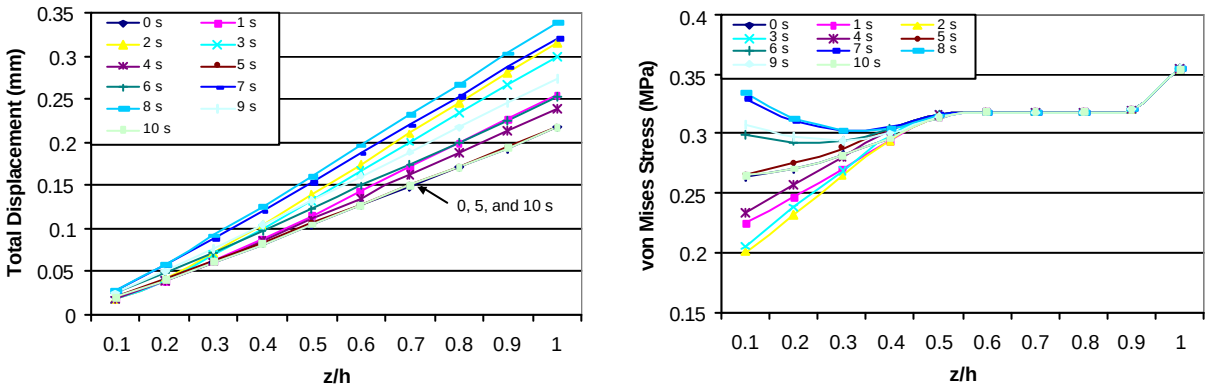

(a) change in total displacement. (b) change in von Mises stress.

Fig. 14 Results showing the changes in total displacement and von Mises stress over the period of the wave at increasing heights on the pile.

4. Conclusions

In this study, the deformation and stresses within an offshore concrete pile under combined structural and wave loading is analysed by the finite element method. A control model is analysed using a specific set of control data, then compared to succeeding models as the pile and loading parameters are changed. The parameters used to complete this study are the structural to static water pressure ratio, the pile radius and the water depth. After compiling and analysing the results from each test, the following conclusions can be made:

- The structural load does have a significant impact on the overall behavior of the pile under the combined loading conditions and must be considered when designing a pile under similar conditions.
- Changing the parameters of the pile and loading condition has a significant impact on the resulting stress distributions and displacements.
- An adequate pile radius should be used to reduce the amount of stress at the critical points.
- The critical failure point can be located in the pile, but will continue to move around the pile over the period of the wave so this must be considered in the design procedure.

A design procedure for a pile considering a structural load only half of the water pressure should not be the same as a design procedure for a structural load of ten times the water pressure. Similarly, a pile designed for a location with a water depth below the mid-height of the pile should not be designed according to the same procedure as location with a water depth of 2/3 the height of the pile. Using the results provided here, more effective design codes can be formulated to take into account the behavior of the pile to a specific structural load to water pressure ratio, as well as to account for a varying loading conditions similar to those adopted in this study.

References

1. M.C. Au, and C.A. Brebbia, "Diffraction of water waves for vertical cylinders using boundary elements", Applied Mathematical Modelling, Vol. 7, April 1983, pp 106-114.
2. S.K. Chakarabarti, A. Tam, "Interaction of waves with large vertical cylinder", Journal of Ship Research, Vol. 19, March 1975, pp 22-23.
3. H. Raman, N. Jothishankar, and P. Venkatanarasaiah, "Nonlinear wave interaction with vertical cylinder of large diameter", Journal of Ship Research, Vol. 21, No. 1, June 1977, pp 120-124.
4. S. Zhu, "Diffraction of short-crested waves around a circular cylinder", Ocean Engineering, Vol. 20, No.4, 1993, pp 389-407.
5. S. Zhu, and G. Moule, "Numerical calculation of forces induced by short-crested waves on a vertical cylinder of arbitrary cross-section", Ocean Engineering, Vol. 21, No. 7, 1994, pp 645-662.
6. W.H. Tang, "Uncertainties in offshore axial pile capacity", Foundation Engineering: Current Principles and Practices, New York, NY, 1989, pp 833-847.
7. R.M. Sorensen, Basic Coastal Engineering, Chapman & Hall, New York, NY, 1997.
8. G+D Computing. Using Strand7: Introduction to the Strand7 finite element analysis system, Sydney, Australia, 1999.

